

1 Localised economic impacts from high 2 temperature disruption days under climate change

3 Authors:

4 Tim Summers (1), Erik Mackie (2, 3), Risa Ueno (3, 5), Charles Simpson (3), J. Scott
5 Hosking (3, 4), Tudor Suciu (6), Andrew Coburn (1), Emily Shuckburgh (2, 6)

6

7 This paper is a non-peer reviewed preprint submitted to EarthArXiv. It has also been
8 submitted to the journal 'Climate Resilience and Sustainability'.

9 Affiliations:

- 10 1. Centre for Risk Studies, Judge Business School, University of Cambridge
- 11 2. Cambridge Zero, University of Cambridge
- 12 3. British Antarctic Survey, NERC
- 13 4. The Alan Turing Institute
- 14 5. Department of Chemistry, University of Cambridge
- 15 6. Department of Computer Science & Technology, University of Cambridge

16 Emails:

17 t.summers@jbs.com.ac.uk
18 erik.mackie@admin.cam.ac.uk
19 risno@bas.ac.uk
20 champs@bas.ac.uk
21 jask@bas.ac.uk
22 ts809@cam.ac.uk
23 andrew.coburn@jbs.cam.ac.uk
24 efs20@cam.ac.uk

25 Twitter:

26 @emilyshuckburgh, @Summertim, @ErikMackie, @scotthosking

27 Address for correspondence:

28
29 Dr T Summers,
30 Centre for Risk Studies,
31 Cambridge Judge Business School,
32 University of Cambridge,
33 Trumpington Street,
34 Cambridge
35 CB2 1AG,
36 UK
37

38 Data availability: Our analysis is based on data available via CEDA's data analysis
39 environment JASMIN <https://help.jasmin.ac.uk/article/189-get-started-with-jasmin> .
40
41

42 Abstract

43 Most studies into the effects of climate change have headline results in the form of a global
44 change in mean temperature. More useful for businesses and governments however are
45 measures of the economic impact, either direct or indirect. We have addressed this by
46 examining how the frequency of exceeding a daily mean temperature threshold changes,
47 defined as “disruption days”, as it is often this exceedance which has the most dramatic
48 impacts on personal or economic behaviour. Our exceedance analysis tackles the resolution
49 of climate change both geographically and temporally, the latter specifically to address the 5-
50 20 year time horizon which can be recognised in business planning.

51 We apply bias correction with quantile mapping to meteorological reanalysis data from
52 ECMWF ERA5 and output from CMIP5 climate model simulations. By determining the daily
53 frequency at which a mean temperature threshold is exceeded in this bias-corrected dataset,
54 we can compare predicted and historic frequencies to estimate the change in the number of
55 disruption days. Furthermore, by combining results from 18 different climate models, we can
56 estimate the likelihood of more extreme events, taking into account model variations. This is
57 useful for worst case scenario planning.

58 Taking the city of Chicago as an example, the expected frequency of years with 40 or more
59 disruption days above the 25°C threshold rises by a factor of four for a time period centred
60 on 2040, compared with a period centred on 2000. Alternately, looking at the change in the
61 number of days at a given likelihood, an example is Shenzhen, where the number of
62 disruption days in a once-per-decade event exceeding the 25°C or 30°C threshold is
63 expected to rise by a factor of four.

64 Superimposing these results onto maps of, for instance, GDP sensitivity or production days
65 lost, will provide more accurate and targeted conclusions for future impacts of climate
66 change. This method of quantifying costs on business-relevant timescales will help
67 businesses and governments properly include risks associated with facilities, plan mitigating
68 actions and make accurate provisions. It can also, for example, inform their disclosure of
69 physical risks under the framework of the Task Force on Climate-related Financial
70 Disclosures. This approach is equally applicable to other weather-related, localised
71 phenomena likely to be impacted by climate change.

72 Keywords:

73 economic, disruption, climate, temperature, bias, correction, exceedance

74 Introduction

75 Human-induced climate change has resulted in over 1.0°C of global warming to-date, when
76 compared with pre-industrial levels (IPCC 2018). The impacts of this warming trend on
77 human and natural systems are already being felt around the world, in part through an
78 increase in the likelihood of extreme weather events such as heatwaves. For example, the
79 recent Siberian heatwave (January - June 2020) has been shown to be at least 600 times
80 more likely as a result of human-induced climate change (Kew et al. 2020), while the
81 probability of the conditions occurring that led to the 2019/2020 Australian bushfires are

82 estimated to have increased by at least 30% since 1900, due to anthropogenic climate
83 change (van Oldenborgh et al. 2020). These risks will increase with future warming.

84 The acute impact of climate change on business and society can be directly observed
85 through changes to the tails of climatic distributions, as extreme events become more likely
86 or more severe. But they are much harder to infer from apparently small changes in central
87 statistics like the rise in the annual global average temperature. Extreme weather events can
88 have adverse financial impacts on businesses through damage to physical assets, disruption
89 or reduction in productivity of operations and supply chains, and impacts to market demand
90 for products and services (Handmer et al. 2012).

91 These risks are of growing concern for businesses, and many corporations are trying to
92 understand how present and future changes in extreme weather risk are likely to affect them.
93 Organisations are under pressure to take action to address environmental, social and
94 corporate governance (ESG) demands, and for strategic and competitive reasons, as well as
95 address regulatory requirements or other liabilities they may face. Mapping the geographical
96 overlap of extreme weather events and business systems is key to providing insight to global
97 corporates of the exposure of their entire value chains to physical climate change risk.

98 These needs are framed by the recommendations of the Task Force for Climate-related
99 Financial Disclosures (TCFD), which has been voluntarily adopted by more than 1,500
100 global organisations as of October 2020 (TCFD 2020). Investors are mobilising to pressure
101 companies to respond to the TCFD recommendations and disclose climate-related risks,
102 with the threat that they will be less inclined to invest in companies that fail to do so (Eccles,
103 2018). Companies that comply with the recommendations will have better strategies to adapt
104 to climate change and may be more able to harness any potential opportunities that climate
105 change presents.

106 The TCFD includes a recommendation to describe the impacts of acute (i.e. extreme)
107 weather events, causing physical risks on an organisation over three time horizons, typically
108 below 5 years, five to ten years and beyond ten years. Organisations' energies are typically
109 more focused on short time-frames that they use to conduct operational, financial, strategic,
110 and capital planning (TCFD 2020). However, the currently available data and model
111 projections of future changes in extreme weather risk often do not suit the requirements of
112 businesses. Organisations are struggling to reconcile the long-term projections of the
113 consequences of a warmer planet in several decades' time with changes in the frequency,
114 severity, and geography of extreme weather events that are already having financial impacts
115 on their businesses.

116 Economic productivity is particularly sensitive to extreme heat and associated hazards,
117 which can affect large regions simultaneously to produce widespread impacts and economic
118 loss (Handmer et al. 2012). These impacts are variable across sectors, and particularly
119 affect those relying on labour-intensive activities such as agriculture, manufacturing, and
120 construction (Zuo et al. 2015, Simpson et al., 2021). Human output is impacted through time
121 loss resulting from the heat-induced health outcomes, or 'absenteeism', as well as
122 reductions in work productivity and capacity, termed 'presenteeism' (Xia et al. 2018).
123 Infrastructure, transportation, and energy systems are also vulnerable to extreme heat, and
124 physical damage or service outages can severely disrupt supply chain activities and markets

125 for products and services. Major cities, where economic activity is concentrated, are also
126 subject to an urban heat island effect and so heat waves are typically more extreme, and
127 can result in large death tolls and significant economic loss (Wouters et al. 2017) (Mora et al.
128 2017).

129 Here we present a geographic resolution of one arc-degree grid squares as a starting point
130 for risk assessment of global business activity, namely supply chains, transportation routes
131 and retail distribution, and to demonstrate a methodology that can be refined and improved.
132 This resolution corresponds to approximately a 110 km square at the equator, and a 110 km
133 by 78 km rectangle at a temperate latitude of 45°.

134 Data and Methods

135 We use climate model outputs from the Coupled Model Intercomparison Project Phase 5
136 (CMIP5) to quantify future changes in extreme temperatures for the period 2020-2059,
137 combined with recent historical data from the European Centre for Medium-Range Weather
138 Forecasts (ECMWF) Re-Analysis (ERA5) for the period 1979-2018 (Hersbach et al. 2020).¹
139 The metric used in this paper is the mean daily temperature. Although daily maximum or
140 minimum temperatures, midday temperatures or other measures might be more appropriate
141 for specific tasks (agricultural yields for instance often depend on minimum as well as
142 maximum temperatures), the mean daily temperature is a good proxy for others and more
143 representative of the overall risk, and thus a good starting point for this generalised study. A
144 subset of 18 of the CMIP5 models is used: details are given in the appendix. For all models,
145 only the RCP4.5 emissions scenarios are used as there is little divergence between the
146 pathways prior to 2060. By the year 2040, the middle of the 2020-2059 period examined in
147 this paper, the RCP4.5 scenario corresponds approximately to a 1.5°C warmer world,
148 compared with pre-industrial temperatures. Information from the historical period is used to
149 identify systematic biases between the climate model simulations and observational data at
150 a local scale and this is used to produce a transfer function to bias correct future projections.

151 A summary of the five-stage approach used is given below, followed by a more detailed
152 description of each step:

- 153 1. ERA5 and CMIP5 data are firstly interpolated onto a common spatial grid.
- 154 2. For each of the models used, at each location, a bias correction to the raw data is
155 calculated based on the observational data. This defines a transfer function that is
156 then used on model predictions to bias-correct each model's future output.
- 157 3. Using the bias-corrected daily mean temperature predictions with specified
158 temperature thresholds, the annual number of days that the mean daily temperature
159 exceeds a defined threshold (the number of "disruption days") is quantified.
- 160 4. The distribution of the number of disruption days is calculated over a 40-year period
161 for each model at each location.
- 162 5. Combining outputs from all models gives an estimate of the likely number of
163 disruption days, for a given temperature threshold, at each location for a specified
164 time period.

¹ Data was accessed through the Centre for Environmental Data Analysis (CEDA), which makes the data available on JASMIN: <https://help.ceda.ac.uk/article/4465-cmip5-data> ; Copernicus Climate Data Store, available from: <https://cds.climate.copernicus.eu/#/search?text=ERA5&type=dataset>

165 Re-gridding

166 ERA5 reanalysis and CMIP5 model outputs are interpolated onto a common spatial grid, a
167 necessity given that different models use different grids. The grid is centred on squares one
168 arc degree wide, between 70°S and 70°N, over land mass. This area is chosen since the
169 majority of economic activity takes place over land mass away from the poles. For coastal
170 locations, the centre of the cell used is the centroid of the land mass, to minimise the
171 influence of the ocean. This results in data being obtained for approximately 18,000
172 geographic locations. While this resolution is high enough for many economic activities, any
173 localised temperature influences (including topographic or urban heat island effect) may be
174 under-represented.

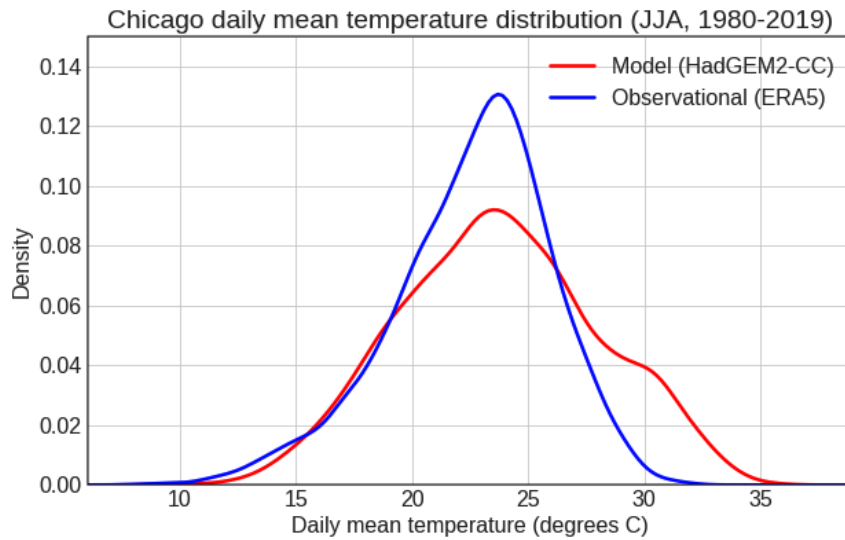
175 Bias correction

176 Statistical bias correction is a widely adopted post-processing procedure applied to climate
177 model simulation outputs to produce location-specific future projections for impact modelling
178 e.g. (Hawkins et al. 2013). This aims to remove the bias arising from model deficiencies and
179 unresolved physical processes in an individual climate model.

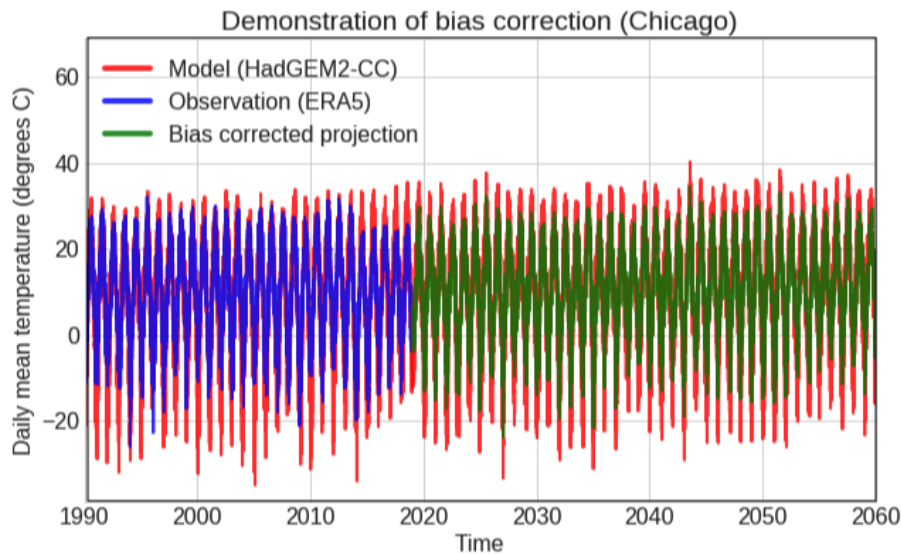
180 In this work, we adopt the quantile mapping method for bias correction, a popular distribution
181 correction technique that has been found to outperform simpler bias correction methods that
182 only account for the mean, or mean and variance of the climate variable (Gudmundsson et
183 al. 2012). Quantile mapping is particularly effective in correcting the tails of a distribution,
184 which is an important consideration in this work concerning extreme events.

185 It has been shown that applying quantile mapping to raw data can artificially alter the trends
186 which can weaken the credibility of the resulting projection, and it has been argued that the
187 climate change signal simulated by the model should be preserved (Haerter et al. 2011),
188 (Maraun 2013). Therefore, we detrend the timeseries as a pre-processing step, and
189 subsequently reintroduce the future model trend after applying quantile mapping. This
190 encourages bias correction to account for daily variability without the long-term trend
191 corrupting the overall distribution. We use a 31-day sliding window over the calendar year to
192 avoid climatological discontinuity and use a linear regression to fit a trend for each window in
193 order to capture the long-term signal that may depend on the time of year, as demonstrated
194 in (Hempel et al. 2013). A second order polynomial is used to capture any acceleration in the
195 future climate change signal, which was found to be more robust than a single linear fit (not
196 shown). As with any statistical procedure, bias correction comes with a set of assumptions
197 that are discussed extensively, e.g. Maraun et al. 2017, Maraun and Widmann 2018.

198 The period 1979 to 2018 inclusive, comprising 40 years of daily data, for which we have
199 overlapping ERA5 measurements and predictions from each CMIP5 model, is used to
200 calibrate the bias correcting transfer function. This is then applied to the future model
201 simulations for the years 2020 to 2059 inclusive to obtain bias-corrected future projections.
202 Transfer functions are derived for each model for every location, a total of approximately
203 330,000. Figure 1 illustrates an example for one location (Chicago) and one model
204 (HadGEM2-CC): the summer daily mean temperature distribution of HadGEM2-CC output
205 and corresponding ERA5 data, illustrating the discrepancy between them (top), and a
206 timeseries of HadGEM2-CC, ERA5 and bias corrected projection (bottom).



207



208

209 Figure 1: Demonstrating the bias correction: comparison of summer (JJA) daily mean
 210 temperature distributions between raw model output (HadGEM2-CC) and ERA5 in
 211 Chicago (top); demonstration of bias correction as a timeseries of raw model output
 212 (HadGEM2-CC), observational data (ERA5) and bias-corrected output (bottom).

213 Distribution of future temperature disruption days

214 The analysis of the bias corrected data examines the 40-year period 2020 - 2059 and makes
 215 statistical predictions for the number of days with temperatures above a defined threshold in
 216 this period. This is what we refer to as the number of “disruption days”.

217 Counting the number of disruption days in each year during the period gives a distribution of
 218 40 points. This can be visualised as an exceedance plot (i.e. 1 – CDF, the cumulative
 219 distribution function), showing, for a given probability, how many days are expected to be
 220 above a particular temperature. Given that the results have been analysed over a 40-year
 221 period, these results can be interpreted as the best estimate for a period centred on 2040,
 222 the midpoint of the analysis (although there is a long-term trend in temperatures over this
 223 period).

224 Given the relatively low granularity of the output (only 40 data points), kernel density
225 estimation (KDE) is used to better visualise the underlying statistical process. The KDE
226 bandwidth used is varied for each location and temperature, and corresponds to 6.7% of the
227 90% - 10% days: best practice for a Gaussian distribution would be approximately 15%
228 (Silverman 1986), but the authors feel that the long tails in this distribution justify a tighter
229 bandwidth.

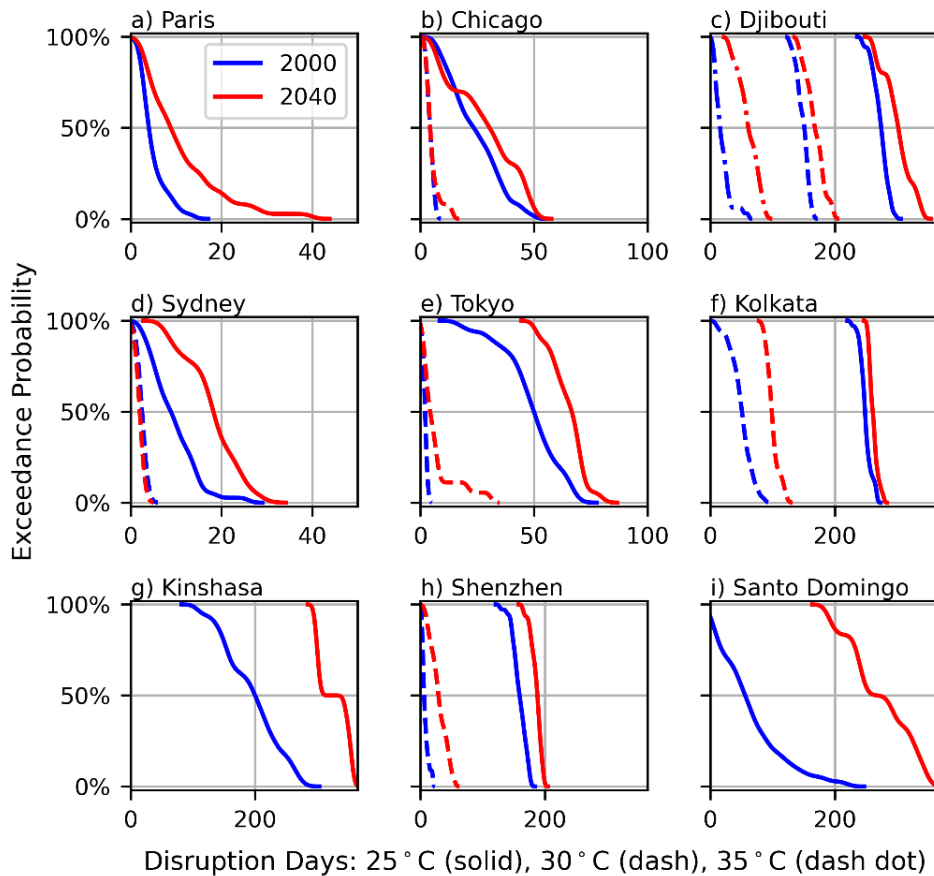
230 Results

231 Interpretation of a single location

232 Figure 2 shows outputs for a single model (HadGEM2-CC, red line, centred on 2040) for
233 nine example locations from our global analysis, with up to three temperature thresholds
234 (25°C, 30°C and 35°C), and compared with the ERA5 historic measurements (blue line,
235 centred on 2000). The nearest city locations to the actual analysed points are given in Table
236 1. These nine example locations were chosen in order to represent a broad geographic
237 spread of locations across all continents (excluding Antarctica).

238 The disruption days metric is based on specified mean daily temperature thresholds (25°C,
239 30°C and 35°C in this case), and the probability of a threshold being exceeded in any given
240 year. This is shown on the vertical axes in Figure 2: for example, 10% exceedance
241 probability corresponds to a once-per-decade event, or 1% corresponds to a once-per-
242 century event. These thresholds and exceedance probabilities can be adapted according to
243 the business assets in question, to match with the acceptable level of risk to the asset
244 operator, or to reflect the relevant regional context.

245 Figure 2 illustrates that the modelled future changes in the number of disruption days vary
246 widely by geographic location. For example, looking at the example of Paris in Figure 2a, we
247 see an increase of between 10 and 20 disruption days at the 25°C threshold (solid line), for
248 low exceedance probabilities (i.e. 1-in-100 or 1-in-10 year events), but only a small increase
249 of just a few disruption days at higher exceedance probabilities. In contrast, for Santo
250 Domingo in Ecuador (Figure 2i), we see a large increase of over 100 disruption days for the
251 25°C threshold at all exceedance probabilities. Kinshasa in DR Congo (Figure 2g) shows
252 similarly large increases in the number of disruption days at the 25°C threshold. The other
253 locations in Figure 2 also show increases in the number of disruption days at the 30°C
254 threshold (dashed line), and for some (e.g. Kolkata, Figure 2f), the modelled increase at the
255 30°C threshold is greater than at the 25°C threshold. For Djibouti (Figure 2c), we see the
256 greatest increase in number of disruption days at the 35°C threshold (dashed-dotted line).
257 Recall that these thresholds illustrate the mean daily temperature, the peak daily
258 temperature will be significantly higher. The global variation in results is also clear from the
259 global maps shown in Figures 4 & 5.



260

261

262

263

Figure 2: Exceedance plot of number of disruption days above three mean daily temperature thresholds (25°C, 30°C and 35°C), for nine locations, from one model (HadGEM2-CC, red), compared with the historic measurements from ERA5 (blue).

Nearest city	Country	Latitude, longitude
Paris	France	48.5 N, 2.5 E
Chicago	USA	41.5 N, 87.5 W
Djibouti	Djibouti	11.5 N, 42.5 E
Sydney	Australia	33.4 S, 151.25 E
Tokyo	Japan	35.5 N, 139.5 E
Kolkata	India	22.5 N, 88.5 E
Kinshasa	D R Congo	4.5 S, 15.5 E
Shenzhen	P R China	22.74 N, 114.42 E
Santo Domingo	Ecuador	0.5 S, 79.5 W

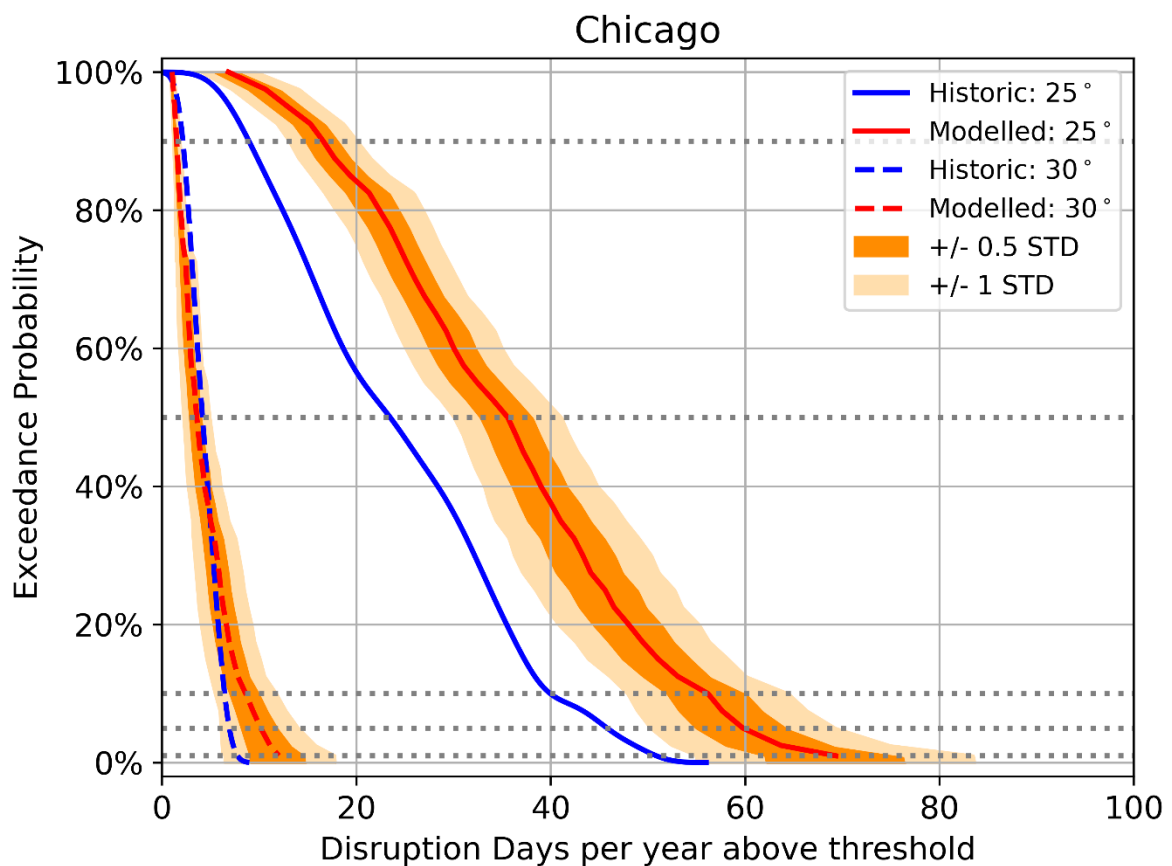
264

265

Table 1: Nearest cities and the exact locations used in the analysis

266 Combining results from all models

267 Each of the 18 models used provides a set of results for each of the approx. 18,000
268 locations. We combine the output from the ensemble of all models to give distributions over
269 the models at each exceedance probability for each temperature threshold. The ensemble-
270 mean provides a “best guess” estimate of the number of disruption days at a particular
271 exceedance probability, while adding a number of standard deviations from the mean
272 provides an indication of a worst-case with a known degree of confidence. Figure 3 shows
273 an example for a single location, the grid cell containing Chicago. The distribution of results
274 between models allows us to give a measure of the assessed likely range (+/- S std) of the
275 prediction around model risk. Statements can be made in the format: ‘At location L, in the
276 period centred on 2040, it is expected that one in N years will have D days disruption at a
277 mean daily temperature above T, with S std of confidence’.



278
279

280 Figure 3: Exceedance plot of number of disruption days above two mean daily
281 temperature thresholds, for one location, with example exceedance probabilities of
282 1%, 5%, 10%, 50% and 90% (grey dotted lines). The ensemble results from all 18
283 bias-corrected models are combined to give statistical measures.

284 For example, referring to the results for Chicago given in Figure 3, we might be interested in
285 a 1-in-10-year scenario, i.e., an exceedance probability, shown on the vertical axis, of 10%.
286 The measurements show that historically there have been approximately 40 days per year,
287 shown on the horizontal axis, where the mean daily temperature has exceeded 25°C (solid
288 blue line): but with the impact of climate change, this is expected to rise to approximately 55

289 days (solid red line). Therefore, we can say: 'In Chicago for the period centred on 2040, we
290 expect every decade there will be one year where 55 days have a mean daily temperature
291 above 25°C, up from 40 days for the period centred on 2000'. The uncertainty between
292 different models can be accounted for by the addition of the following statement: 'there is a
293 16% chance that every decade one year will have 64 days exceeding this threshold'
294 (corresponding to +1 std). This is essential for planning worst case scenarios and takes
295 account of model risk by incorporating an ensemble of results from different groups.

296 Although the change in absolute number of days may be quite small (55 disruption days
297 rather than 40), in a location which is historically ill-prepared for high temperatures, each day
298 can cause a significant cost and an increase in the fraction of days lost could be very
299 significant. One example might be locations in temperate regions that generally do not have
300 air conditioning, where the investment needed to install widespread building cooling capacity
301 would be very significant.

302 Another interpretation is to find the change in frequency for a given number of disruption
303 days. Referring again to Figure 3, there is approximately 10% probability (i.e. 1-in-10 year
304 expectation) of 40 disruption days with a mean daily temperature above 25°C at the baseline
305 2000 condition. Under climate change, for the period centred on 2040 the same number of
306 disruption days is expected with about 38% likelihood, approximately 4-in-10 years. Thus,
307 we can expect approximately four times the number of years with this number of disruption
308 days.

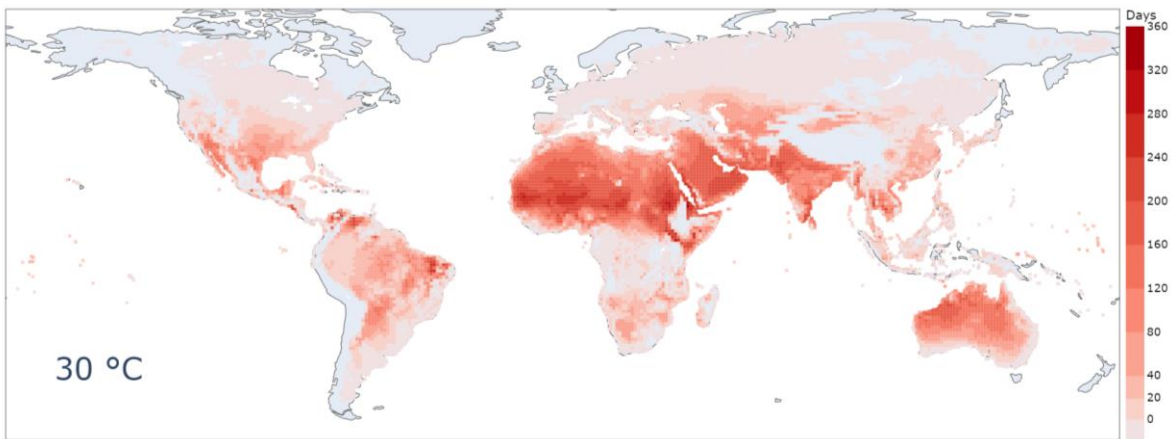
309 This is often a more impactful way to understand the predictions. Risk and operation
310 managers and senior executives might be tempted to regard a 1-in-10 year expected loss as
311 simply a 'risk of doing business' which will generally be smoothed over with preceding and
312 following 'normal' years. If, however this loss approaches a 1-in-2 frequency, it will need to
313 be addressed, mitigated or provisioned. We believe that this method of presenting the
314 impacts of climate change is likely to promote meaningful change from operators and
315 owners of economic assets.

316 Global depiction of results

317 The examples above demonstrate the presented methodology for individual cities, with a
318 moderate temperature threshold. However, this technique is intended for a global application
319 to enable risk analysis of the exposures of global activities and value chains: the example of
320 Chicago above is also applicable to any global location. It is acknowledged that the use of an
321 absolute temperature threshold (e.g. 30°C) has been criticised for not taking into account
322 climate variability (Zuo et al. 2015). However, we suggest that the application of critical
323 thresholds of disruption in this way is a useful method to assess global exposures in a
324 systematic way. Differences in the coping capacity of a specific region or locale to extreme
325 heat can be accounted for through variation of the vulnerability component of a risk
326 calculation.

327 Figure 4 shows a global map of the absolute number of disruption days over the 30°C
328 threshold for the 2020-2059 period, at a 10% exceedance probability (one year in 10). For
329 each global location, the mean exceedance from all 18 of the bias corrected models is used.
330 It is clear from the map that for large parts of Saharan Africa, the Middle East and India, in

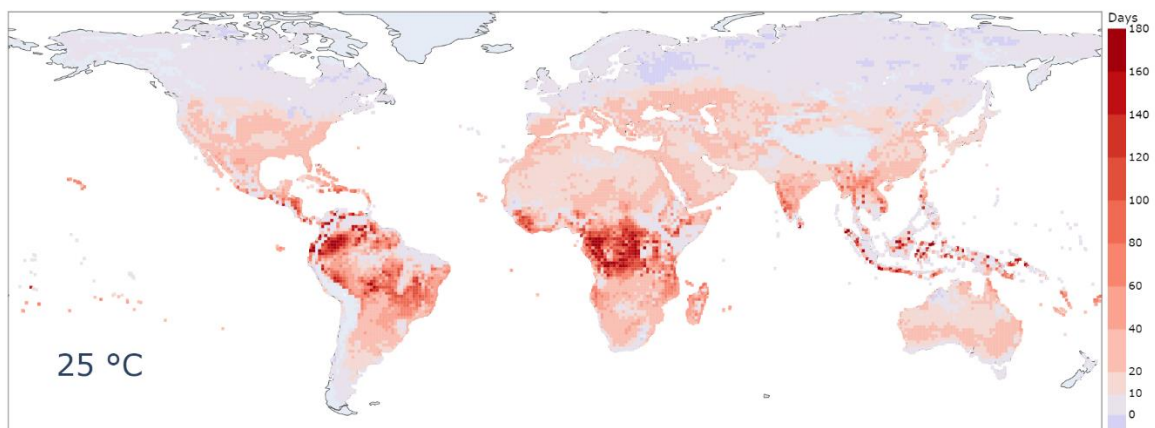
331 the period centred on 2040, it is expected that one-in-ten years will have a large number of
332 more than 200 disruption days per year over the 30°C threshold, with some regions
333 experiencing up to 360 disruption days per year. A large number of disruption days is also
334 expected in Australia. Some parts of South America, in particular in the Amazon Basin, also
335 show a large number of disruption days. In other regions globally, including Europe, Sub-
336 Saharan Africa and North America, the absolute number of expected disruption days per
337 year at the 30°C threshold tends to be lower. However, while the absolute number of
338 disruption days may seem low in some regions, the *increase* in the number of disruption
339 days per year may still be higher. This is discussed in Figure 5.



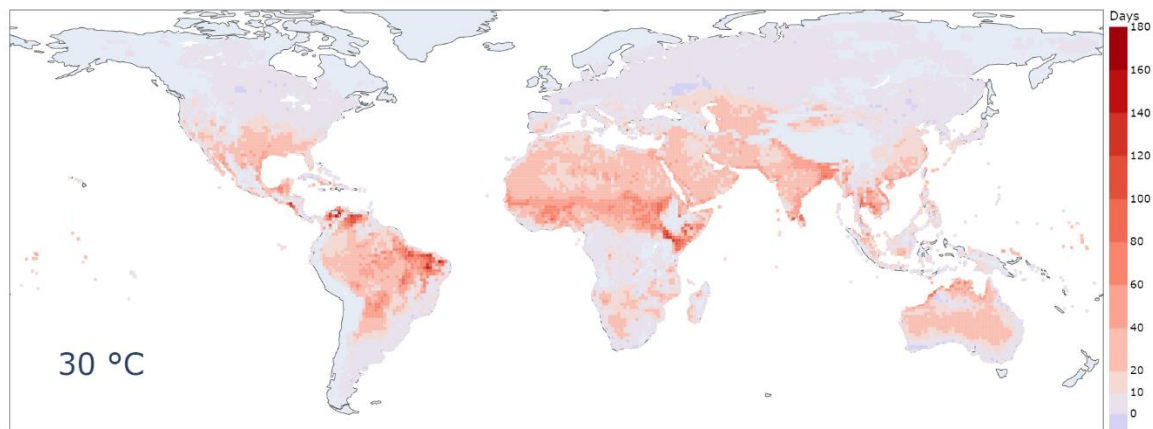
340
341 Figure 4: Absolute number of daily mean disruption days per year over the 30°C temperature
342 threshold for the 2020-2059 period, at a one-year-in-ten exceedance probability.
343

344 Figure 5 shows global maps of the expected increase in the number of disruption days from
345 1979-2018 to 2020-2059, using the threshold of mean daily temperature exceeding 25°C,
346 30°C and 35°C, with a 10% probability of exceedance (i.e. one year each decade).
347 Differences in the impact between regions expected as a result of climate change can easily
348 be seen. For example, Central America and sub-Saharan Africa have a high increase in
349 daily mean 25°C disruption days, but the greatest impact at 35°C is in Saharan Africa and
350 the Middle East, which likely are close to exceeding lower temperature thresholds for most
351 days at historic conditions (illustrated for the example of Djibouti in Figure 2c). This
352 distinction is important, as a temperature threshold that is impactful in one region of the
353 world may be less relevant in another, demonstrating the need for regionally specific
354 thresholds.

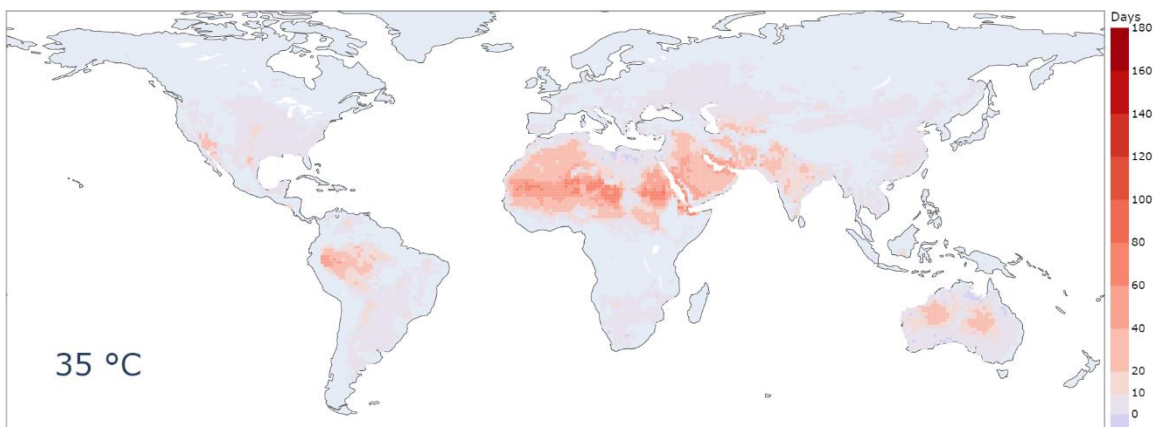
355



356



357



358

359 Figure 5: Expected increase in the number of daily mean 25°C (top), 30°C (middle)
 360 and 35°C (bottom) disruption days from 1979-2018 to 2020-2059, at a one-year-in-
 361 ten exceedance probability, mean from all 18 bias-corrected models.

362 Maps such as these can be generated for any temperature or probability threshold,
 363 incorporating if necessary a measure to account for uncertainty between the climate models,
 364 by including a number of standard deviations from the mean between models at each
 365 location, as illustrated for a single location (Chicago) in Figure 3. This approach can be
 366 readily applied to risk assessment in a variety of domains, through analysis of the extreme
 367 heat hazard against exposures and vulnerabilities of specific sectors, such as agriculture
 368 (where agricultural risk models are used to calculate production disruption) or manufacturing
 369 (e.g. to assess rates of absenteeism/presenteeism, reduction of output, energy demands
 370 and air conditioning loads, etc.).

371 Aggregated global results

372 Although the primary focus of this paper is on providing localised estimations of the change
 373 in disruption days, it is also interesting to get a broad measure of the global change in
 374 disruption days. To do so, we divide the globe into three zones by latitude: 0° to 23.5°
 375 ('tropical'), 23.5° to 35.5° ('sub-tropical') and 35.5° to 70° ('temperate'). For each land-mass
 376 grid square in each zone and at each temperature threshold, we calculate the mean of the
 377 baseline number of disruption days and the mean of the increase in disruption days
 378 expected from 1979-2018 to 2020-2059. The results are shown in Table 2.

379

Threshold temp (daily mean)	Zone	Mean baseline number of disruption days for 1979-2018	Mean increase in number of disruption days from 1979-2018 to 2020-2059
25°C	Tropical	237	39
	Sub-tropical	125	20
	Temperate	16	8
30°C	Tropical	51	26
	Sub-tropical	56	20
	Temperate	5	6
35°C	Tropical	17	19
	Sub-tropical	19	12
	Temperate	1.3	4.2

380 Table 2: Mean number of disruption days, and mean increase, for three latitude zones at
381 three temperature thresholds

382 This averaged analysis of course hides a large amount of local data: some localities will
383 have a much larger increase in the number of disruption days and some may have no
384 increase or even a slight decrease (for example some regions of Russia and Canada show a
385 decrease in Figure 5).

386 Given the wide distribution in the increase in the number of disruption days, a more
387 informative way to analyse the data is to ask what fraction of locations in each zone have
388 more than a given number of days increase. We show this fraction in Table 3 for the same
389 temperature thresholds and latitude zones, for 10 and 30 days.

Threshold temp (daily mean)	Zone	Fraction of locations with more than 10 disruption days increase	Fraction of locations with more than 30 disruption days increase
25°C	Tropical	77%	44%
	Sub-tropical	82%	12%
	Temperate	20%	1%
30°C	Tropical	64%	28%
	Sub-tropical	66%	16%
	Temperate	7%	0%
35°C	Tropical	24%	12%
	Sub-tropical	29%	7%
	Temperate	1%	0%

390 Table 3: Fractional increase in the number of locations predicted to have 10 and 30
391 additional disruption days, for three latitude zones at three temperature thresholds

392 Tropical regions are impacted the most with highest fraction of locations suffering 30
393 additional days. For 10 days, sub-tropical regions are approximately equally affected, with
394 temperate latitudes the least impacted. It is worth remembering though that temperate
395 regions may have the biggest financial sensitivity to the disruption days, since many
396 locations will be relatively poorly prepared.

397

398 Discussion

399 Although in some cases the absolute increase in the number of disruption days in the results
400 discussed above is relatively small, we must remember that:

- 401 • This analysis is performed on daily mean temperatures, so a daily peak temperature
402 will be significantly higher.
- 403 • Economic processes slow down very rapidly with rising temperature, so (for instance)
404 the prospect of a threefold increase in the number of economically unproductive days
405 would be highly impactful.
- 406 • The strong variation between locations (illustrated in Figures 2 & 5) shows that this
407 mean increase includes many locations with a much higher increase.
- 408 • Some locations will be less prepared than others. For example, housing and
409 workspaces in many temperate locations do not have air cooling. As a result, an
410 increase in the number of days at even a low temperature threshold could have a
411 higher economic impact than at a sub-tropical location, where at least there is a
412 higher level of preparedness to hot days.

413 Localised Economic Impacts

414 Extreme climate events are known to cause devastating damage, both in human lives and in
415 financial assets. The future 'climate value at risk' of global financial assets is US\$2.5 trillion
416 in the 'business-as-usual' scenario, while the 99th percentile of the possible outcomes gives
417 the value of approximately US\$24.2 trillion (Dietz et al. 2016). In addition, climate-economic
418 models show that losses from climate change may reach 23% of the global gross product by
419 the end of the 2100 (Klusak et al., 2021; Burke et al., 2015). Over the past 40 years (since
420 1980), estimations show that weather-related natural disasters alone caused losses of
421 around US\$4.2 trillion and claimed approximately 1 million lives (Munich Re, 2021).

422 Heatwaves have shown increasing trends in frequency, duration and cumulative heat since
423 the mid-twentieth century, and have also shown signs of acceleration of those trends in the
424 presence of global warming (Perkins-Kirkpatrick and Lewis, 2020). Those upward trends can
425 be seen in the recent past of such events - the major European heat waves of 2003 and
426 2019 were just 16 years apart but were estimated to be 1-in-450 years and 1-in-283 years
427 events respectively (Munich Re, 2004; Ma et al., 2020). Those types of events can be
428 catastrophic for people, countries and businesses, especially if mitigation plans are not in
429 place. The 2003 European heat wave claimed an estimated 35,000 lives, 14,947 out of
430 those in France alone, a country without a strategy against heat waves at the time (Larsen
431 2003, Poumadère et al., 2005). Estimates of the financial cost for this event alone are
432 around US\$13 billion, mostly in agricultural costs, which is believed to be a conservative
433 estimate as crops were not usually insured in Europe in 2003 (Munich Re, 2004; De Bono et
434 al., 2004).

435 Providing economic loss calculations due to future heat waves is outside the scope of this
436 paper, but the methods and results showcased in this study can provide a good baseline for
437 such estimations. For example, making an assumption that the 1995 Chicago heat wave
438 was a 1-in-100 years event (Karl and Knight, 1997) and the fact that this event is part of the
439 1979-2018 timeseries, one can use our disruption days framework to estimate the probability

440 of a similar event arising in the 2040-centered period. Reading from Figure 3, in terms of the
441 same number of disruption days (both 25°C and 30°C thresholds), the probability of having a
442 similar event would increase to 10% (or 1-in-10 years). This result is limited by the
443 aforementioned assumption, but also by the assumption that the ‘disruption days per year’
444 metric is perfectly correlated with the emergence of heat waves. The lack of higher precision
445 in distributions of this metric can also have an effect on this result as the smallest increment
446 in our exceedance probability plots is 2.5%, while the event is assumed to have a probability
447 of 1%. However, this result does show the potential of this type of analysis for the mitigation
448 of future extreme weather events.

449 By knowing the sensitivity to temperatures and the geographic distribution of their
450 operations, it becomes feasible for an organization or business to quantify their expected
451 total financial loss due to temperature disruption days. This could be essential for
452 provisioning, insurance or risk reporting, including TCFD disclosures. It also lays the
453 foundations for planning strategic responses to physical climate change risk.

454 Future Work

455 The procedures described in this paper give the first stage of assessing a financial cost at a
456 relatively local resolution from extreme temperature effects, expressed as “disruption days”.
457 However, it needs to be followed by assessments at a local level of economic vulnerability to
458 disruption days. These could be as simple as “the airport will close if the mean daily
459 temperature is above 35°C” or “the cost of electricity generation for the region rises by
460 US\$50 million for each day above 30°C”. At the other extreme, a complex, multi-location
461 operation could assess operations at each location, and apply these vulnerabilities to the
462 disruption days calculated here to give a total expected additional cost. By combining all
463 significant economic activity in a region and estimating vulnerability to extreme weather, it
464 would be possible for a local or national government to estimate the gross effect of
465 temperature disruption days on their economy. A multinational company with economically
466 productive assets spread over many locations could do the same.

467 The general approach used in this study (re-gridding at relatively fine spatial granularity, bias
468 correction of individual models, calculation of the disruption days for each model at each
469 location, followed by ensemble averaging over models to get model risk statistics) can
470 equally well be applied to other extreme weather features which are likely to be affected by
471 climate change, and could be the subject of future work:

- 472
- 473 ● Precipitation. Droughts and flooding have profound effects on many natural and
474 human activities, not least agriculture.
- 475 ● Multivariate analysis of compound risks. For example, the impacts of humidity
476 combined with temperature, or drought combined with high temperature.
- 477 ● Low temperature thresholds. Frost days, for example, can limit economic activity in
478 some temperate regions, where freezing temperatures are relatively rare and
479 preparedness is low.
- 480 ● Quantifying maximum or minimum daily temperatures, rather than mean daily
481 temperatures, might also be interesting as many activities are more accurately limited
482 by daily extremes rather than mean temperatures.
- 483

484 The methodological analysis presented in this paper could be improved in future studies as
485 and when new datasets and methods become available. In terms of data preparation and
486 pre-analysis, machine learning methods show great promise in improving existing bias
487 correction techniques, and such new methods could be applied to repeat and improve our
488 analysis presented here. While this study has focussed on the use of model results from the
489 CMIP5 generation of climate models, the newly available generation of CMIP6 models have
490 a higher spatial resolution and would allow for the approach in this paper to be repeated with
491 finer geographic grids.

492 Conclusion

493 Using multi-model, bias-corrected results from CMIP5 climate models we estimate the
494 frequency of daily mean temperatures exceeding certain temperature thresholds on
495 “disruption days”, at given locations for a future period centred on 2040, compared with
496 historical observations from ERA5 centred on 2000. Since it is often the exceedance over a
497 threshold, rather than simply the mean annual temperature, that is the determining factor for
498 economic activity, this approach is expected to be a better indicator on the effect of climate
499 change on human and economic activity.

500 Our results allow for the estimation of the increase in the number of disruption days
501 exceeding a certain temperature threshold for a given location and exceedance probability.
502 For example, in Chicago one can expect that by 2040, every decade there will be one year
503 where 55 days have a mean daily temperature above 25°C, up from 40 days for the period
504 centred on 2000. Another way to read the results is that Chicago can expect a fourfold
505 increase in the number of years with at least 40 disruption days above the 25°C threshold by
506 2040.

507 Globally, our results also show that there is broad variation in the modelled increase in
508 number of disruption days, for different locations, temperature thresholds and exceedance
509 probabilities. Central America and Sub-Saharan Africa show the largest increases in number
510 of disruption days at the 25°C temperature threshold, while the greatest increases in
511 disruption days exceeding 35°C are seen in Saharan Africa and the Middle East.

512 By combining these results with the sensitivities of economic activities to temperature
513 thresholds, it becomes possible to estimate the financial impact of climate change on a wide
514 variety of businesses. Examples are logistics (frequently disrupted by weather extremes),
515 outdoor work (where human productivity rapidly falls with temperature) and agricultural
516 yields (which typically fall once a crop-dependant temperature threshold is passed).

517 By knowing locations and the nature of activities through an organisation, it will be possible
518 to estimate, with a given level of confidence over model risk, the financial impact of climate
519 change related changes in temperature.

520

521 Acknowledgement

522 The authors would like to express gratitude to Professor Daniel Ralph and Mr Oliver
523 Carpenter at The Centre for Risk Studies, University of Cambridge, Judge Business School.

524

525 Appendix

526 The CMIP5 models used are: ACCESS1-3, BNU-ESM, CMCC-CMS, CNRM-CM5, CSIRO-
527 Mk3-6, GFDL-CM3, GFDL-ESM2G, GFDL-ESM2M, HadGEM2-CC, HadGEM2-ES, IPSL-
528 CM5A-LR, IPSL-CM5A-MR, IPSL-CM5B-LR, MPI-ESM-LR, MPI-ESM_MR, NorESM1-M,
529 bcc-csm1-1 and inmcm4. A small number of other models were not included either because
530 they had been superseded by later models from the same research group or because of
531 data incompatibilities.

532

533 References

- 534 Burke, Marshall, Solomon M. Hsiang, and Edward Miguel. "Global non-linear effect of
535 temperature on economic production." *Nature* 527, no. 7577 (2015): 235-239.
- 536 Ciavarella. (2020). *Prolonged Siberian heat of 2020*. Retrieved 10 25, 2020, from
537 [https://www.worldweatherattribution.org/wp-content/uploads/WWA-Prolonged-heat-](https://www.worldweatherattribution.org/wp-content/uploads/WWA-Prolonged-heat-Siberia-2020.pdf)
538 [Siberia-2020.pdf](https://www.worldweatherattribution.org/wp-content/uploads/WWA-Prolonged-heat-Siberia-2020.pdf)
- 539 Dietz, Simon, Alex Bowen, Charlie Dixon, and Philip Gradwell. "'Climate value at
540 risk' of global financial assets." *Nature Climate Change* 6, no. 7 (2016):
541 676-679.
- 542 De Bono, Andréa, Pascal Peduzzi, Stéphane Kluser, and Gregory Giuliani. "Impacts of
543 summer 2003 heat wave in Europe." (2004).
- 544 Eccles, R. & Krzus, M. (2018). Why Companies Should Report Financial Risks From
545 Climate Change. *MIT Sloan Management Review*, 59(3), 1-6.
- 546 Gudmundsson, Lukas, John Bjørnar Bremnes, Jan Haugen, and T. Skaugen. 2012.
547 'Technical Note: Downscaling RCM Precipitation to the Station Scale Using Quantile
548 Mapping – A Comparison of Methods'. *Hydrology and Earth System Sciences*
549 *Discussions* 9 (May): 6185–6201. <https://doi.org/10.5194/hessd-9-6185-2012>.
- 550 Haerter, J. O., S. Hagemann, C. Moseley, and C. Piani. 2011. 'Climate Model Bias
551 Correction and the Role of Timescales'. *Hydrology and Earth System Sciences* 15
552 (3): 1065–79. <https://doi.org/10.5194/hess-15-1065-2011>.
- 553 Handmer, John, Yasushi Honda, Zbigniew W. Kundzewicz, Nigel Arnell, Gerardo Benito,
554 Jerry Hatfield, Ismail Fadl Mohamed, et al. 2012. 'Changes in Impacts of Climate
555 Extremes: Human Systems and Ecosystems'. In *Managing the Risks of Extreme*
556 *Events and Disasters to Advance Climate Change Adaptation*, edited by Christopher
557 B. Field, Vicente Barros, Thomas F. Stocker, and Qin Dahe, 231–90. Cambridge:
558 Cambridge University Press. <https://doi.org/10.1017/CBO9781139177245.007>.
- 559 Hawkins, Ed, Thomas M. Osborne, Chun Kit Ho, and Andrew J. Challinor. 2013. 'Calibration
560 and Bias Correction of Climate Projections for Crop Modelling: An Idealised Case
561 Study over Europe'. *Agricultural and Forest Meteorology*, Agricultural prediction using
562 climate model ensembles, 170 (March): 19–31.
563 <https://doi.org/10.1016/j.agrformet.2012.04.007>.
- 564 Hempel, Sabrina, Katja Frieler, Lila Warszawski, Jacob Schewe, and Franziska Piontek.
565 2013. 'A Trend-Preserving Bias Correction – The ISI-MIP Approach'. *Earth System*
566 *Dynamics Discussions* 4 (January): 49. <https://doi.org/10.5194/esdd-4-49-2013>.
- 567 Hersbach, Hans, Bill Bell, Paul Berrisford, Shoji Hirahara, András Horányi, Joaquín
568 Muñoz-Sabater, Julien Nicolas, et al. 2020. 'The ERA5 Global Reanalysis'. *Quarterly*
569 *Journal of the Royal Meteorological Society* 146 (730): 1999–2049.
570 <https://doi.org/10.1002/qj.3803>.
- 571 IPCC. 2018. 'Summary for Policymakers — Global Warming of 1.5 °C'. 2018.
572 <https://www.ipcc.ch/sr15/chapter/spm/>.

573 Karl, Thomas R., and Richard W. Knight. "The 1995 Chicago heat wave: How likely is a
574 recurrence?." *Bulletin of the American Meteorological Society* 78, no. 6 (1997): 1107-
575 1120.

576 Kew, Sarah, Sjoukje Philip, Geert Jan van Oldenborgh, Amalie Skålevåg, and Philip Lorenz.
577 2020. 'Prolonged Siberian Heat of 2020', 35.

578 Larsen, Janet. "Record heat wave in Europe takes 35,000 lives: Far greater losses may lie
579 ahead." Earth Policy Institute (2003).

580 Poumadere, Marc, Claire Mays, Sophie Le Mer, and Russell Blong. "The 2003 heat wave in
581 France: dangerous climate change here and now." *Risk Analysis: an International*
582 *Journal* 25, no. 6 (2005): 1483-1494.

583 Klusak, Patrycja, Matthew Agarwala, Matt Burke, Moritz Kraemer, and Kamiar Mohaddes.
584 "Rising temperatures, falling ratings: The effect of climate change on sovereign
585 creditworthiness." (2021).

586 Ma, Feng, Xing Yuan, Yang Jiao, and Peng Ji. "Unprecedented Europe heat in June–July
587 2019: risk in the historical and future context." *Geophysical Research Letters* 47, no.
588 11 (2020): e2020GL087809.

589 Maraun, Douglas. 2013. 'Bias Correction, Quantile Mapping, and Downscaling: Revisiting
590 the Inflation Issue'. *Journal of Climate* 26 (6): 2137–43. [https://doi.org/10.1175/JCLI-](https://doi.org/10.1175/JCLI-D-12-00821.1)
591 [D-12-00821.1](https://doi.org/10.1175/JCLI-D-12-00821.1).

592 Maraun, Douglas, Theodore G. Shepherd, Martin Widmann, Giuseppe Zappa, Daniel
593 Walton, José M. Gutiérrez, Stefan Hagemann, et al. 2017. 'Towards Process-
594 Informed Bias Correction of Climate Change Simulations'. *Nature Climate Change* 7
595 (11): 764–73. <https://doi.org/10.1038/nclimate3418>.

596 Maraun, Douglas, and Martin Widmann. 2018. *Statistical Downscaling and Bias Correction*
597 *for Climate Research*. Cambridge: Cambridge University Press.
598 <https://doi.org/10.1017/9781107588783>.

599 Mora, Camilo, Bénédicte Dousset, Iain R. Caldwell, Farrah E. Powell, Rollan C. Geronimo,
600 Coral R. Bielecki, Chelsie W. W. Counsell, et al. 2017. 'Global Risk of Deadly Heat'.
601 *Nature Climate Change* 7 (7): 501–6. <https://doi.org/10.1038/nclimate3322>.

602 Munich Re. "TOPICS geo 2003." Mü nchener RÜ ckversicherungs-Gesellschaft, Munich
603 (2004).

604 Oldenborgh, Geert Jan van, Folmer Krikken, Sophie Lewis, Nicholas J. Leach, Flavio
605 Lehner, Kate R. Saunders, Michiel van Weele, et al. 2020. 'Attribution of the
606 Australian Bushfire Risk to Anthropogenic Climate Change'. *Natural Hazards and*
607 *Earth System Sciences Discussions*, March, 1–46. [https://doi.org/10.5194/nhess-](https://doi.org/10.5194/nhess-2020-69)
608 [2020-69](https://doi.org/10.5194/nhess-2020-69).

609 Silverman, B.W. (1986). *Density Estimation for Statistics and Data Analysis*. London:
610 Chapman & Hall/CRC. p. 45. ISBN 978-0-412-24620-3.

611 Simpson, C, Hosking, J S, Mitchell, D, Betts, R A, and Shuckburgh, E. 2021. 'Regional
612 Disparities in Climate Risk to Rice Labour and Food Security'. *Submitted to*
613 *Environmental Research Letters*, Preprint: <https://doi.org/10.31223/X5SW3N>.

614 TCFD. 2020. '2020 Status Report'. Task Force on Climate-Related Financial Disclosures.
615 2020. [https://www.fsb.org/2020/10/2020-status-report-task-force-on-climate-related-](https://www.fsb.org/2020/10/2020-status-report-task-force-on-climate-related-financial-disclosures/)
616 [financial-disclosures/](https://www.fsb.org/2020/10/2020-status-report-task-force-on-climate-related-financial-disclosures/).

617 ———. 2020. 'Support TCFD'. *Task Force on Climate-Related Financial Disclosures* (blog).
618 2020. <https://www.fsb-tcf.org/support-tcf/>.

619 Wouters, Hendrik, Koen De Ridder, Lien Poelmans, Patrick Willems, Johan Brouwers,
620 Parisa Hosseinzadehtalaei, Hossein Tabari, Sam Vanden Broucke, Nicole P. M.
621 van Lipzig, and Matthias Demuzere. 2017. 'Heat Stress Increase under Climate
622 Change Twice as Large in Cities as in Rural Areas: A Study for a Densely Populated
623 Midlatitude Maritime Region'. *Geophysical Research Letters* 44 (17): 8997–9007.
624 <https://doi.org/10.1002/2017GL074889>.

625 Xia, Yang, Yuan Li, Dabo Guan, David Mendoza Tinoco, Jiangjiang Xia, Zhongwei Yan, Jun
626 Yang, Qiyong Liu, and Hong Huo. 2018. 'Assessment of the Economic Impacts of

627 Heat Waves: A Case Study of Nanjing, China'. *Journal of Cleaner Production* 171
628 (January): 811–19. <https://doi.org/10.1016/j.jclepro.2017.10.069>.
629 Zuo, Jian, Stephen Pullen, Jasmine Palmer, Helen Bennetts, Nicholas Chileshe, and Tony
630 Ma. 2015. 'Impacts of Heat Waves and Corresponding Measures: A Review'. *Journal*
631 *of Cleaner Production* 92 (April): 1–12. <https://doi.org/10.1016/j.jclepro.2014.12.078>.

632